

CASFISH: CRISPR/Cas9-mediated in situ labeling of genomic loci in fixed cells

Wulan Deng^{a,1}, Xinghua Shi^a, Robert Tjian^{a,b}, Timothée Lionnet^a, and Robert H. Singer^{a,c,d,1}

^aTranscription Imaging Consortium, Janelia Research Campus, Howard Hughes Medical Institute, Ashburn, VA 20147; ^bDepartment of Molecular and Cell Biology, University of California, Berkeley, CA 94707; ^cDepartment of Anatomy and Structural Biology, Albert Einstein College of Medicine, Bronx, NY 10461; and ^dGruss-Lipper Biophotonics Center, Albert Einstein College of Medicine, Bronx, NY 10461

Contributed by Robert H. Singer, August 11, 2015 (sent for review July 15, 2015; reviewed by Joseph G. Gall, Arjun Raj, and Xiaowei Zhuang)

Direct visualization of genomic loci in the 3D nucleus is important for understanding the spatial organization of the genome and its association with gene expression. Various DNA FISH methods have been developed in the past decades, all involving denaturing dsDNA and hybridizing fluorescent nucleic acid probes. Here we report a novel approach that uses in vitro constituted nuclease-deficient clustered regularly interspaced short palindromic repeats (CRISPR)/CRISPR-associated caspase 9 (Cas9) complexes as probes to label sequence-specific genomic loci fluorescently without global DNA denaturation (Cas9-mediated fluorescence in situ hybridization, CASFISH). Using fluorescently labeled nuclease-deficient Cas9 (dCas9) protein assembled with various single-guide RNA (sgRNA), we demonstrated rapid and robust labeling of repetitive DNA elements in pericentromere, centromere, G-rich telomere, and coding gene loci. Assembling dCas9 with an array of sgRNAs tiling arbitrary target loci, we were able to visualize nonrepetitive genomic sequences. The dCas9/sgRNA binary complex is stable and binds its target DNA with high affinity, allowing sequential or simultaneous probing of multiple targets. CASFISH assays using differently colored dCas9/sgRNA complexes allow multicolor labeling of target loci in cells. In addition, the CASFISH assay is remarkably rapid under optimal conditions and is applicable for detection in primary tissue sections. This rapid, robust, less disruptive, and cost-effective technology adds a valuable tool for basic research and genetic diagnosis.

that the dCas9/sgRNA binary complex could be repurposed as a highly specific and efficient enzymatic probe for labeling DNA without global DNA denaturation, which is generated by heat or chemical treatments in DNA FISH protocols (Fig. 1A). Here we report the method exploiting the CRISPR/Cas9 system for DNA FISH studies allowing multicolored and expansive labeling of genomic DNA sequences in cells and tissues.

Results

To produce fluorescently labeled dCas9 protein, we constructed a dCas9 fusion protein that contains a hexahistidine affinity tag at the N terminus and a Halo tag at the C terminus. The Halo tag can be labeled efficiently and covalently by Halo ligands conjugated to a variety of organic fluorescent dyes for different imaging purposes (10). We purified recombinant dCas9 fusion protein expressed in *Escherichia coli* and labeled the protein with Halo ligands conjugated with Janelia Fluor 646 (JF646) (11). (All fluorochromes are listed in Table S1.) We first chose to test our strategy on the highly repetitive major satellite (MajSat) sequences at murine pericentromeric regions (12) and thus generated a 5'-DY547 (Cy3 alternative)-labeled sgRNA (sgMajSat) (Fig. 1B). Equal molar amounts of purified JF646-dCas9 and DY547-sgMajSat were incubated together to form the dCas9/sgMajSat complex and then were applied to mouse embryonic fibroblasts (MEFs) that were fixed with methanol/acetic acid solution. Within 30 min of incubation, dCas9/sgMajSat probes effectively hybridized to the target satellite DNA in pericentromeres (Fig. 1C). Images from the DY547 channel that detects sgMajSat, the JF646 channel that detects dCas9 protein, and the DAPI channel generated a colocalized pattern of the pericentromeres in nuclei.

Cas9 | FISH | genome organization | CRISPR | Halo

In cells, genomic DNA is highly folded and organized in three dimensions. The spatial organization of chromatin in the nucleus and the relative positions of distinct chromatin regions are tightly associated with gene regulation in normal development and disease (1). DNA FISH has been widely used to visualize sequence-specific chromatin domains or genes for research and diagnostic purposes (2). Despite continuous improvements, DNA FISH requires harsh treatments of heat and formamide to denature dsDNA to allow probe hybridization, thus running the risk of affecting the integrity of the biological structure and genome organization. DNA FISH also is limited in detection resolution with BAC probes and by the high cost of oligo probes (3). Thus there is an opportunity to develop simpler, more efficient and robust in situ imaging of cellular DNA.

The type II clustered regularly interspaced short palindromic repeats (CRISPR)-CRISPR-associated caspase 9 (Cas9) system derived from *Streptococcus pyogenes* has become a revolutionary tool for targeted genome editing (4), and its nuclease-deficient derivatives (dCas9) also are used for control of gene expression (5) and visualization of genomic loci in live cells (6–8) through fusion with a transcription-regulation domain or a fluorescent protein, respectively. Inherent multiplexing features offered by the CRISPR system hold great promise for applications in high-throughput assays. However, expanding its use in studying the spatial dynamics of any given genomic loci remains challenging because of the need for multicolored labels and efficient transduction of tens to hundreds of single-guide RNAs (sgRNAs) (6). In vitro studies of the CRISPR system indicated that Cas9/sgRNA had a strong and stable affinity for its target DNA (9). We hypothesized

Significance

We have derived a new technology for the detection of genes within undisturbed nuclei of fixed cells and tissues. Previous approaches have used fluorescent DNA probes to hybridize to genes of interest, requiring treatment of heat and disruptive chemicals that distort the natural organization of the nucleus. Instead, we have used a bacterial protein, CRISPR (clustered regularly interspaced short palindromic repeats), combined with an RNA sequence as probes to find the genes of interest in the intact genome. This approach preserves the spatial relationships of the genetic elements, which are important for understanding gene expression, and the process is remarkably rapid (15 min), convenient, and can be used directly on tissues for diagnosis of disease.

Author contributions: W.D., T.L., and R.H.S. designed research; W.D. and X.S. performed research; W.D., R.T., T.L., and R.H.S. analyzed data; and W.D. and R.H.S. wrote the paper. Reviewers: J.G.G., Carnegie Institution of Washington; A.R., University of Pennsylvania; and X.Z., Harvard University and Howard Hughes Medical Institute.

The authors declare no conflict of interest.

Freely available online through the PNAS open access option.

¹To whom correspondence may be addressed. Email: dengw@janelia.hhmi.org or singerr@janelia.hhmi.org.

This article contains supporting information online at www.pnas.org/lookup/suppl/doi:10.1073/pnas.1515692112/-DCSupplemental.

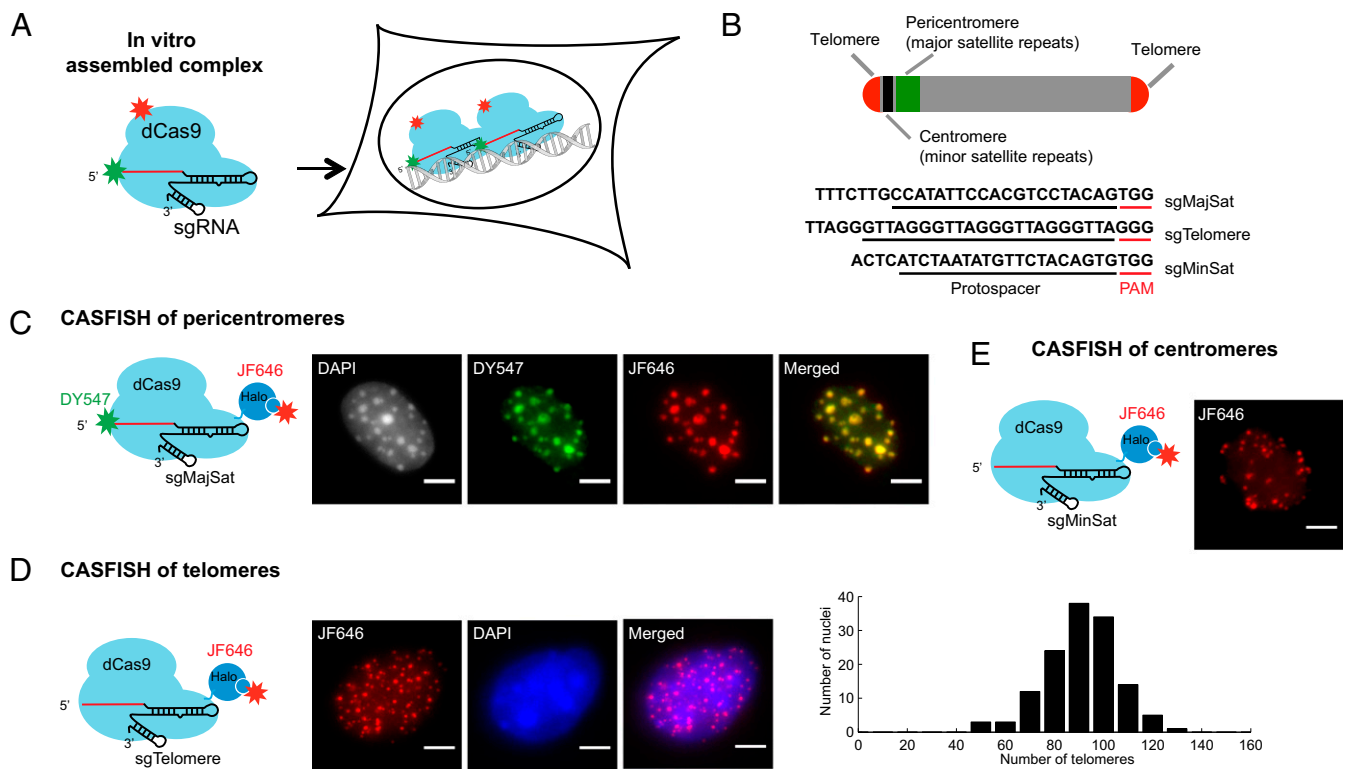


Fig. 1. In vitro assembled dCas9/sgRNA fluorescently labels genomic DNA in cells. (A) Schematic of the CASFISH strategy. (B, Upper) Relative positions of indicated DNA elements on a murine chromosome. (B, Lower) sgRNA sequences as indicated. (C) CASFISH against pericentromeres in MEFs using the indicated fluorescent dCas9/sgMajSat probe assembled in vitro. dCas9 was labeled by JF646, and sgMajSat was labeled with DY547. Fluorescent images were taken with indicated filter settings and are pseudocolored for visualization purposes. (D, Left) CASFISH against telomeres in MEFs using the indicated fluorescent dCas9/sgTelomere complex. (D, Right) Histogram of the number of detected telomeres per cell; $n = 134$ cells. (E) CASFISH in MEF cells against minor satellite elements in centromeres. Maximum projection of z-stacks is shown. (Scale bars, 5 μ M.)

Pericentromeres were of various sizes and numbers, as observed in live MEF cells coexpressing dCas9-halo and sgMajSat (Fig. S14). Staining of pericentromeres by the fluorescent dCas9/sgMajSat complex was verified further by dCas9 staining with an independent sgRNA (sgMajSat-2) targeting the other strand of the major satellite sequence (Fig. S1B) and by its colocalization with heterochromatin protein 1 alpha (HP1 α) immunofluorescence staining (Fig. S1C). In contrast, JF646-dCas9 alone or incubated with the backbone hairpin portion of sgMajSat lacking a target complementary sequence failed to generate any specific staining (Fig. S1D), indicating that dCas9/sgMajSat-mediated staining of pericentromeres was sequence-specific. DY547-sgMajSat alone did not hybridize with the target major satellite DNA, suggesting that the target DNA was not denatured during the Cas9-mediated FISH (CASFISH) procedure and that the observed signal was not caused simply by RNA–DNA hybridization independent of dCas9 (Fig. S1D). To demonstrate dCas9-mediated fluorescent staining with an independent labeling method, we engineered a genetically encoded aldehyde tag to the N terminus of dCas9 protein and labeled the aldehyde-tagged dCas9 with Cy5 hydrazide (Cy5_{HZ}) (13). The Cy5-labeled dCas9 protein assembled with DY547-sgMajSat generated the same specific staining of pericentromeres as JF646-labeled dCas9 protein (Fig. S2). In summary, these results demonstrated that in vitro assembled fluorescent dCas9/sgRNA complex could label its genomic DNA target sequences in cells effectively and specifically. We therefore named the method “CRISPR/Cas9-mediated FISH,” CASFISH.

The synthesis of fluorochrome-conjugated sgRNA probes (~110 nt) is costly, whereas labeling of the Halo tag is efficient and cost-effective; thus we developed a strategy of assembling fluorescent dCas9-Halo and unlabeled sgRNA for CASFISH. Specifically, we labeled dCas9-Halo protein through Halo ligands

providing flexibility in the choice of fluorochromes and used T7 polymerase to synthesize sgRNA in vitro, a solution combining low cost and scalability for multiplexing. dCas9-Halo proteins labeled with both tested fluorochromes [JF549 and JF646 (11)] retained their activity, as demonstrated by successful CASFISH imaging and specific binding to target DNA in vitro (see below). Assembling labeled dCas9-Halo with T7-synthesized sgRNA, we successfully stained various DNA targets including telomeres, minor satellites, and a gene array containing repeated MS2-binding sequences (Fig. 1D and E and Fig. S34). The number of detected telomeres was in agreement with the number of chromosomes in MEF cells by cytogenetic analysis (Fig. 1D and Fig. S3B and C). Telomere sequences are G-rich and have a higher melting temperature than regular genomic DNA. Although conventional DNA FISH of telomeres requires peptide nucleic acid probes for hybridization (14), the CASFISH probe detected telomeres effectively with unmodified sgRNA, indicating CASFISH's superiority to DNA FISH in detecting G-rich sequences. Thus, we established a cost-effective and convenient pipeline for synthesizing fluorescent CASFISH probes for customized sequences.

Simultaneous imaging of multiple chromatin domains or genes is critical for studying chromatin interactions. To explore the possibility of using CASFISH to detect multiple DNA targets simultaneously, we first investigated the binding of CASFISH probes to target DNA by electrophoretic mobility shift assays (EMSA). Using fluorescently labeled dCas9 protein, sgMajSat, and its target DNA, we found that dCas9 protein formed a binary complex with sgMajSat and a tertiary complex upon the addition of target DNA. These two complexes migrated on the gel as distinct bands away from free dCas9, free sgMajSat, or free target DNA (Fig. S44). As expected, dCas9 showed no detectable interaction with target DNA in the absence of sgMajSat. To examine the

stability of dCas9/sgMajSat binding to its target DNA, we carried out competition assays by adding excessive amounts of unlabeled target DNA to a preformed tertiary complex of JF549-dCas9/sgMajSat/Cy5-DNA. We found that incubation with increasing amounts of competitor DNA did not displace the Cy5-DNA from the preformed tertiary complex, as indicated by unchanged Cy5 fluorescence intensity of the tertiary complex even in the presence

of a 100-fold excess of competitor DNA (Fig. 2A). Incubating preassembled tertiary complex with 30-fold of unlabeled competitor DNA for up to 1.5 h did not dissociate preformed tertiary complex either (Fig. S4B). In line with previous findings (9), these results demonstrated that, once bound to its DNA substrate, the Cas9/sgRNA/DNA complex is exceptionally stable. This prominent feature would allow a strategy of sequential CASFISH

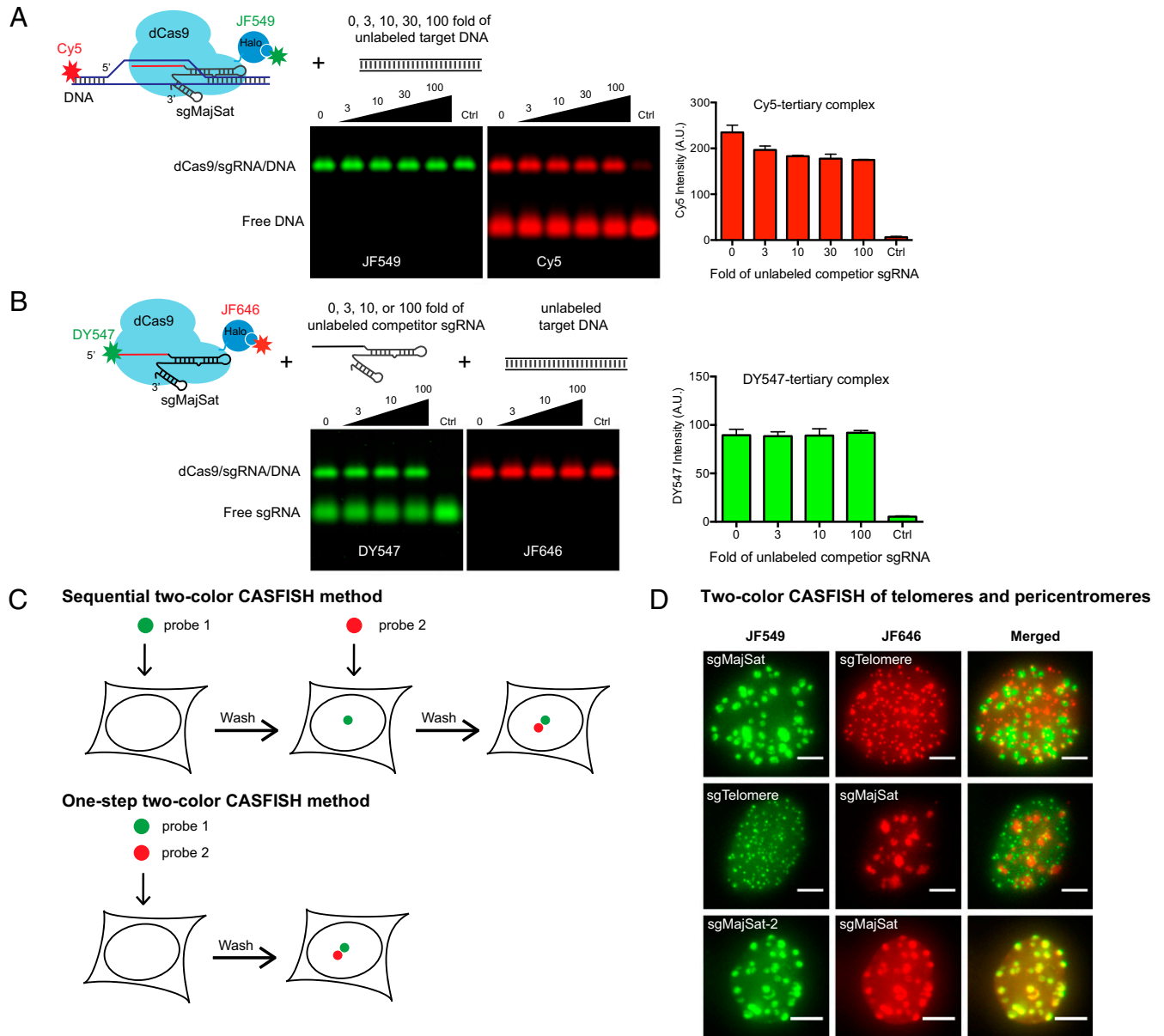


Fig. 2. Two-color CASFISH. (A) Competition EMSA assessing the stability of the tertiary complex. (Left) The indicated fluorescent tertiary complex was assembled in solution and further incubated in 37 °C for 15 min with indicated fold-amounts of unlabeled sgMajSat target DNA as competitor. (Right) The fluorescent intensity of the bands of the tertiary complex plotted as a histogram. The stability of the complex is evident from the lack of competition. The control lane (ctrl) indicates the reaction product from a mixture of Cy5 DNA and 30-fold of unlabeled target DNA with dCas9/sgRNA binary complex. As expected, only a small fraction of Cy5-DNA was incorporated into the dCas9 tertiary complex. (B) Competition EMSAs assessing the stability of the binary complex. (Left) The indicated fluorescent binary complex was assembled at room temperature for 10 min and incubated further with the indicated fold-amounts of unlabeled sgMajSat at room temperature for 10 min. Unlabeled target DNA was added to the solution subsequently to form a tertiary complex followed by gel electrophoresis. (Right) The DY547 intensity of the bands of the tertiary complex plotted as a histogram. The stability of the binary complex of dCas9 and DY547-sgMajSat is evident from the lack of competition. The control lane (ctrl) indicates the reaction product from the binary complex formed by a mixture of DY547-sgMajSat and 100-fold of unlabeled sgMajSat with dCas9 protein. As expected, only a small fraction of DY547-sgMajSat was incorporated into the dCas9 tertiary complex. (C) Schematic of two-color CASFISH methods. (D) Fluorescent imaging of sequential CASFISH against pericentromeres and telomeres in MEFs using the indicated JF549- or JF646-labeled dCas9 proteins and unlabeled sgRNAs. Results from sequential CASFISH are similar to those from one-step method. Maximum projection of z-stacks is shown. (Scale bars, 5 μ m.) Error bars represent the SD of three independent experiments.

by subjecting cells to multiple rounds of CASFISH assays using probes labeled with different fluorochromes and targeting different DNA sequences.

To explore the possibility of applying multiple dCas9/sgRNA species in one step for multicolor imaging, we assessed the stability of the binary complex by sgRNA competition assay. We found that increasing amounts of competitor unlabeled sgRNA up to 100-fold did not displace the DY547-sgRNA from preassembled fluorescent dCas9/sgRNA, as indicated by the unchanged DY547 fluorescence intensity of the dCas9 complex (Fig. 2B). In contrast, adding unlabeled sgRNA competitor before the formation of the binary complex substantially reduced the incorporation of DY547-sgRNA to the dCas9 complex. These results demonstrated the high stability of the binary complex and the feasibility of one-step multicolor CASFISH. Therefore, we tested two methods for multicolor CASFISH: sequential rounds of CASFISH or a one-step application of multiple probes (Fig. 2C). Using JF549-dCas9/sgMajSat and JF646-dCas9/sgTelomere probes, we produced two-color imaging of pericentromeres and telomeres in cells with either the sequential CASFISH method (Fig. 2D) or the one-step method in which the two color probes are applied to the cell simultaneously (Fig. S5). There was no detectable cross-reactivity between the two imaging channels in either case. Probes with switched fluorescent labels gave the same results. As expected, CASFISH using two different sgRNAs targeting sgMajSat and sgMajSat-2 showed identical patterns (Fig. 2D). Thus we demonstrated that CASFISH could be used for imaging multiple sequence-specific genomic regions with multiple colors.

The major satellite and telomere sequences contain hundreds to thousands of repeats for sgRNA targeting. To assess the sensitivity of CASFISH, we tested sgRNAs against DNA substrates with lower copy numbers at the level of tens to hundreds. The human mucin 4 (*MUC4*) and mucin 1 (*MUC1*) genes contain repetitive sequences that have been imaged successfully in live cells with dCas9-EGFP (6). CASFISH using sgRNA against the ~400 copies of the target in exon 2 of the *MUC4* gene (sgMUC4-E2)

and ~45 copies of the target in intron 3 (sgMUC4-I1) detected prominent fluorescent puncta in all examined HeLa cell nuclei using either JF549- or JF646-labeled dCas9 protein (Fig. 3A and Fig. S6A). There are three fluorescent puncta in the majority of cells, as expected for the three copies of *MUC4* loci in interphase HeLa cells (Fig. 3B). We also observed that labeling appeared weaker in sister chromatids (Fig. S6B, puncta 1 and 2) than in replicating sites in the same cells (Fig. S6B, puncta 3 and 4). Two-color sequential CASFISH using these two sgRNA produced puncta in close proximity, verifying that the signal was specific to *MUC4* genes. Based on the fraction of loci labeled in both colors, we estimate the detection efficiency to be $\geq 94\%$. As a control, sequential CASFISH of the *MUC4* and *MUC1* genes (sgMUC4-I1 and sgMUC1-E1) showed distinct locations of these two genes in the nuclei (Fig. 3C), revealing no detectable cross-reactivity between sequential rounds of CASFISH probing. In summary, these results demonstrated that CASFISH is robust and efficient for the simultaneous and multiplexing labeling of multiple given genomic DNA sequences.

To explore the ability of CASFISH to image nonrepetitive genomic loci, we synthesized in vitro 73 sgRNAs tiling the 5-kb nonrepetitive region in the first intron of *MUC4* gene (sgMUC4-tiling) (6). CASFISH probes assembled by the sgRNA mixture and JF646-labeled dCas9 protein were applied to fixed HeLa cells. We observed specific labeling of *MUC4* genes in cells, as verified by proximally localized puncta from a second round of the CASFISH assay using JF549-dCas9/sgMUC4-I1 targeting its repetitive intron 3 (Fig. 3D). We found that CASFISH using sgMUC4-tiling had lower labeling efficiency and higher background than labeling with sgMUC4-I1. Similar observations were made in the live-cell dCas9 imaging (6), suggesting that further understanding and optimization on sgRNA targeting efficiency are needed to improve the imaging of genomic DNA by Cas9.

A diagnostic procedure would be facilitated by a rapid and robust assay for genomic sequences present in tissue. To test whether CASFISH can be applied to tissue sections, we prepared

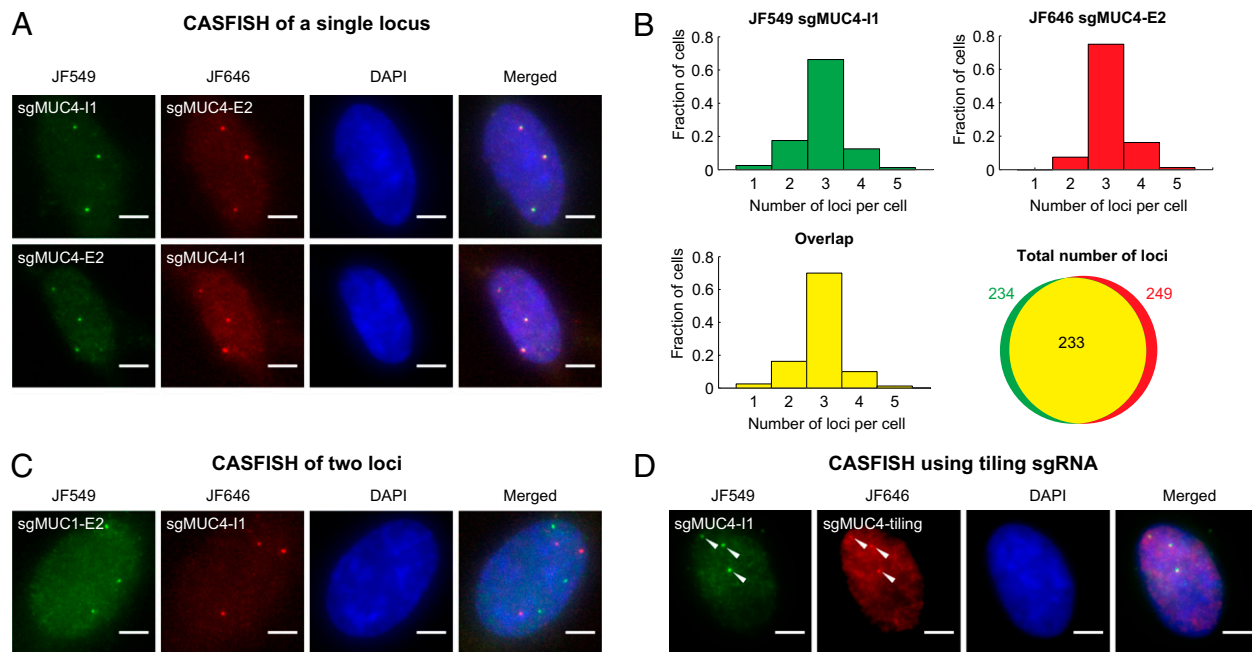
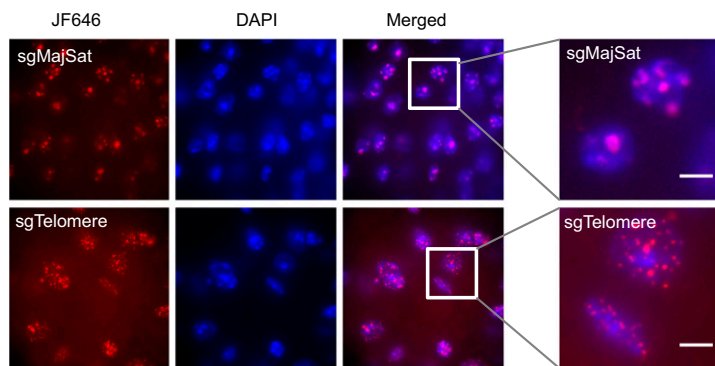


Fig. 3. CASFISH imaging of endogenous coding genes in human cells. (A) Fluorescent imaging of sequential CASFISH targeting two repetitive DNA sequences within intron 3 (sgMUC4-I1) or exon 2 (sgMUC4-E2) of the *MUC4* gene. (B) Quantification of the number of *MUC4* loci per cell and the total number of loci stained by sequential CASFISH against sgMUC4-I1 (green) and sgMUC4-E2 (red) as in A. $n = 80$ cells. Loci labeled by both probes are colored yellow. (C) Fluorescent imaging of sequential CASFISH against the *MUC4* and *MUC1* genes. (D) Sequential CASFISH against repetitive intron 3 (sgMUC4-I1) and nonrepetitive intron 1 (sgMUC4-tiling) of the *MUC4* gene. White arrowheads denote the labeled *MUC4* genes. dCas9 was labeled by JF549 or JF646, as indicated. Maximum projection of z-stacks is shown. (Scale bars, 5 μM .)

A CASFISH on mouse adult brain section



B Fast CASFISH against MUC4 gene

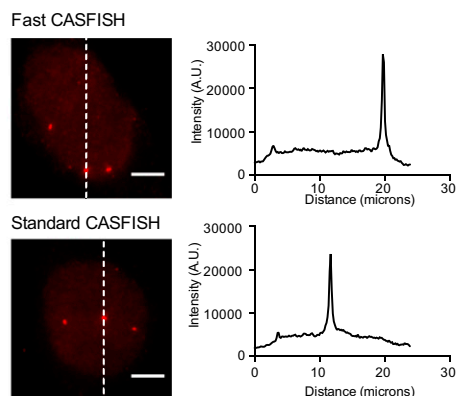


Fig. 4. CASFISH imaging on a tissue section and a fast CASFISH protocol. (A) CASFISH of mouse cryostat brain sections against major satellites and telomeres as indicated. (B, Left) Fifteen-minute and standard CASFISH of the *MUC4* gene in HeLa cells. (B, Right) Intensity profiles across the labeled loci as indicated by the dotted lines on the left panel. dCas9 were labeled by JF646. Maximum projection of z-stacks is shown. (Scale bars, 5 μ M.)

cryostat sections of adult mouse brain and proceeded with CASFISH assays against pericentromeres and telomeres. The dCas9/sgRNA probes penetrated to 15 μ m of the brain sections and efficiently labeled their targets in all examined cells (Fig. 4A). We envision that rapid detection of genomic elements by CASFISH could be advantageous in various scenarios, such as a rapid genetic diagnosis and detection of infectious agents. To derive an even more rapid CASFISH protocol, we reduced the reaction time of each step and achieved a 15-min protocol (5-min fixation and concurrent 5-min binary complex assembly, 5-min DNA binding, and 5-min washing between steps) using sgMUC-E2 as an example. The rapid protocol achieved robust labeling for the *MUC4* gene, with most cells having three labeled puncta, as expected (Fig. 4B). The fluorescent intensity of the labeled locus was similar to that obtained by the standard protocol. These results suggested that CASFISH could be a rapid and robust method for visualizing specific genomic elements in cells and primary tissue. We expect that a similar procedure could be developed for detection of RNA (15).

Discussion

The CASFISH assay is rapid, cost-effective, and convenient (Table 1). First, CASFISH takes advantage of the CRISPR-based mechanism for rapid DNA hybridization. This enzymatic probe is more efficient than the nuclei-acid-only probe of DNA FISH that requires heat and formamide treatment to denature dsDNA. Thus, while DNA FISH takes hours or longer, CASFISH can be as fast as 15 min under optimized conditions. Second, the mild conditions of CASFISH (room temperature and 37 $^{\circ}$ C) can better preserve cell morphology and DNA structure, and thus CASFISH can be a useful tool for studying genome organization combined with single-molecule superresolution imaging (16). Third, the two-component nature of CASFISH probes provides

great potential for multiplexing and room for further engineering (Fig. S7). Halo tagging of dCas9, as demonstrated in this study, allows the ease and flexibility of fluorescent labeling for various imaging purposes. A single reagent of labeled dCas9 protein can be assembled with a number of customized unlabeled sgRNAs at minimal cost. CASFISH therefore can be used to interrogate multiple targets with multiple single colors or with combinatory color codes, facilitating studies of spatial relationships of multiple distinct genomic loci. The fast-binding kinetics of CASFISH probes to targets and the mild reaction conditions would allow highly multiplexed DNA profiling in single cells (17). In addition, the protein moiety of CASFISH probes provides room for exploring other labeling methods and incorporating multiple fluorochromes per molecule to achieve higher sensitivity and specificity. Fourth, CASFISH holds great potential for applications. CASFISH can be advantageous in detecting “difficult” DNA FISH sequences as exemplified by G-rich telomeres. CASFISH can be potentially advantageous in detecting subtle DNA variations such as SNPs because the sgRNA sequence composition near the protospacer adjacent motif (PAM) is sensitive to permutation (18). The CASFISH strategy allows delivery of fluorescent dCas9 protein coupled with unlimited numbers of sgRNA, thereby allowing the labeling of gene loci and chromatin domain of any given size. In principle, customized CASFISH probes can be delivered to live cells via direct microinjection or protein delivery methods to allow studies of native chromatin organization. CASFISH is rapid and applicable to primary tissue, thus offering advantages for rapid genetic diagnosis such as the detection of DNA translocations. The CASFISH assay also could be expanded to orthogonal CRISPR systems (19), allowing a wide range of reagent development and providing an opportunity for developing combinatorial, multiplexed, multicolor imaging systems.

Table 1. Comparison of CASFISH with DNA FISH and live Cas9 imaging

	DNA FISH	Live Cas9 imaging	CASFISH
Probe	Nucleic acid probe	Genetically coded dCas9/sgRNA	In vitro assembled dCas9/sgRNA
Difficulty of probe generation	Reliable synthesis	Variable and time-consuming	Reliable synthesis
Experiment duration	Hours to days	Immediately	Minutes to 1 h
Color	Multicolor	One color per CRISPR system	Multicolor per CRISPR system
High-throughput multiplexing	Yes	Challenging	Yes
Global DNA denaturation	Yes	No	No
Fixed cell imaging	Yes	No	Yes
Live cell imaging	No	Yes	Possible
Tissue imaging	Yes	Possible	Yes

Materials and Methods

dCas9 Constructs and Purification. The *S. pyogenes* Cas9 gene containing the double nuclease mutation (D10A and H840A; dCas9) was cloned into PET302/N (Invitrogen) with an N-terminal hexahistidine affinity tag and a C-terminal Halo tag. A construct with an additional N-terminal aldehyde tag was generated for aldehyde-specific Cy5 labeling (13). All dCas9 fusion proteins were expressed and purified through a three-step FPLC purification protocol as described (*SI Material and Methods*) (20).

dCas9 Fluorescent Labeling. For Halo domain labeling, fluorescent Halo ligands (JF549 and JF646) were mixed in protein samples at ratio of 8:1 and reacted at room temperature for 30 min followed by incubation at 4 °C overnight. The dCas9-Halo with an aldehyde tag was fluorescently labeled with Cy5 hydrazide (GE Healthcare) as described (13). The excessive unreacted fluorescent Halo ligand or Cy5 hydrazide was removed using 40-K molecular weight cut off (MWCO) Zeba spin desalting columns (Thermo Scientific). Protein was eluted in storage buffer containing 50 mM Hepes (pH 7.5), 150 mM KCl, 1 mM Tris(2-carboxyethyl)phosphine (TCEP), and 10% (vol/vol) glycerol, snap frozen in liquid nitrogen, and stored at –80 °C. Protein concentration and labeling efficiency were calculated from absorption spectrum and extinction coefficients according to Beer's laws.

sgRNA Synthesis. The DY547-labeled sgMajSat was generated by splint ligation of two fragments: 36 synthetic nucleotides 5' of sgMajSat with DY547 (GE Dharmacon), and 77 nucleotides 3' of sgMajSat transcribed and purified with T7. The unlabeled sgRNAs were synthesized in vitro by T7 RNA polymerase (MEGAscript T7 Kit; Life Technologies) using DNA templates with the following sequence, 5'-TAATACGACTCACTATAGGN_{17–28}GTTTAAG-AGCTATGCTGGAAACAGCATAGCAAGTTTAAATAAGGCTAGTCCGTTATCAACT-GAAAAAGTGGCACCAGTCCGGTGC-3'. The template contains a T7 promoter-binding sequence (underlined), the sgRNA target (GGN_{17–28}) (bold), and the sgRNA backbone as reported (6). The T7 template DNA was synthesized by either gBlock (Integrated DNA Technologies) or PCR reactions. Produced sgRNAs were purified by MEGAclear Transcription Clean-Up Kit (Life Technologies), and the quality was verified by 10% denaturing PAGE. Related sequences are listed in [Tables S2–S4](#).

Cell Culture and Brain Section Preparation. MEFs and HeLa cells were cultured in DMEM without Phenol-red (Gibco) supplemented with 10% FBS and 1% penicillin/streptomycin. Cytogenetic analysis of MEF cells was performed by Cell Line Genetics. Cryostat sections were prepared from freshly frozen adult mouse brain with a slice thickness of ~20 μM.

CASFISH. Unless indicated, the standard CASFISH protocol is as follows: Cells cultured on 35-mm MatTek dishes or tissue sections were fixed at –20 °C for 20 min in a prechilled solution of methanol and acetic acid at a 1:1 ratio. Samples were washed three times (5 min each washing) with PBS with gentle shaking, followed by incubation for 15 min at 37 °C in blocking/reaction buffer [20 mM Hepes (pH 7.5), 100 mM KCl, 5 mM MgCl₂, freshly added

1 mM DTT, 5% (vol/vol) glycerol, 1% BSA, and 0.1% TWEEN-20]. To assemble CASFISH probes, fluorescently labeled dCas9 protein (5–25 nM) was mixed with labeled or unlabeled sgRNA at molar ratio of 1:1 or 1:4, respectively, in blocking/reaction buffer and was incubated at room temperature for 10 min and stored on ice before the next step. Five nM of fluorescent dCas9 protein was used for CASFISH against *MUC4* repetitive DNA elements. For all other CASFISH experiments, 25 nM dCas9 protein was used. The assembled dCas9/sgRNA was applied on preblocked cells and incubated for 5–30 min at 37 °C. The reaction was terminated by the removal of the dCas9/sgRNA solution and washing three times with blocking/reaction buffer. CASFISH samples of sgMUC4-tiling were washed further in buffer containing 20 mM Hepes (pH 7.5), 300 mM NaCl, 3 M urea, and 1.1% (vol/vol) Nonidet P-40. The short CASFISH protocol was modified to the following procedures: Cells were fixed for 5 min at –20 °C, rinsed three times with PBS, subjected to the preincubated (5 min) dCas9 and sgRNA mixture for 5 min at 37 °C, and again rinsed three times with PBS. All samples were stained with 0.5 μg/mL DAPI for 5 min before imaging.

EMSA Assay. dCas9 protein and sgRNA were incubated together at room temperature for 10 min to examine the binary complex and subsequently were incubated with target DNA at 37 °C for 15 min to examine the tertiary complex. For the competition assay, an additional binary or tertiary complex reaction was performed after the addition of the competitor molecules. Resulting reaction mixtures were subjected to electrophoresis of 1% agarose gel in 1× Tris/borate/EDTA buffer containing 5 mM MgCl₂ and were imaged with GE Typhoon Trio+ Imagers.

Microscopy and Image Analysis. All CASFISH samples were imaged on an inverted microscope (Nikon Eclipse Ti) equipped with a 100× oil-immersion objective (Nikon CFI Plan Apo VC 100× Oil, NA 1.4) and an EM CCD (Andor iXon Ultra 897). DAPI, JF549, or JF646 labeling was imaged using a white light excitation system (SOLA light engine; Lumencor) in conjunction with the proper filter cubes sets (DAPI-11608-NTE-Zero, LF561/LP-A-NTE, or Cy5-3040C-NTE-Zero, respectively; Semrock). JF549 or JF646 labeling also was imaged using laser excitation [561 nm (Cobolt Jive) or 637 nm (Vortran Stradus), respectively] in conjunction with a multiband dichroic (Di01-R405/488/561/635; Semrock). Proper emission filters for JF549 or JF646 (FF01-593/40 or FF01-676/37; Semrock) were placed in front of the camera. Z-stacks were collected at step size of 0.2 μm for 30–40 slices to image the entire nucleus. Images were processed using ImageJ (21).

ACKNOWLEDGMENTS. We thank L. Lavis for generously providing Janelia Fluor-conjugated Halo ligands; L. Xie for providing the PET302/N-dCas9-Halo construct; Z. Zhang and G. Henry for experimental discussions; B. Mehl for assistance with microscopy; W. Hu and L. Witkowsky for assistance with protein purification; A. Hu and R. Gong for preparing mouse brain cryostat sections; and J. Doudna for helpful discussions. Funding was provided by the Howard Hughes Medical Institute. W.D. received support from the Helen Hay Whitney Foundation.

- Hübner MR, Eckersley-Maslin MA, Spector DL (2013) Chromatin organization and transcriptional regulation. *Curr Opin Genet Dev* 23(2):89–95.
- Levsky JM, Singer RH (2003) Fluorescence in situ hybridization: Past, present and future. *J Cell Sci* 116(Pt 14):2833–2838.
- Beliveau BJ, et al. (2012) Versatile design and synthesis platform for visualizing genomes with Oligopaint FISH probes. *Proc Natl Acad Sci USA* 109(52):21301–21306.
- Sternberg SH, Doudna JA (2015) Expanding the Biologist's Toolkit with CRISPR-Cas9. *Mol Cell* 58(4):568–574.
- Mali P, Esvelt KM, Church GM (2013) Cas9 as a versatile tool for engineering biology. *Nat Methods* 10(10):957–963.
- Chen B, et al. (2013) Dynamic imaging of genomic loci in living human cells by an optimized CRISPR/Cas system. *Cell* 155(7):1479–1491.
- Tanenbaum ME, Gilbert LA, Qi LS, Weissman JS, Vale RD (2014) A protein-tagging system for signal amplification in gene expression and fluorescence imaging. *Cell* 159(3):635–646.
- Ma H, et al. (2015) Multicolor CRISPR labeling of chromosomal loci in human cells. *Proc Natl Acad Sci USA* 112(10):3002–3007.
- Sternberg SH, Redding S, Jinek M, Greene EC, Doudna JA (2014) DNA interrogation by the CRISPR RNA-guided endonuclease Cas9. *Nature*.
- Encell LP, et al. (2012) Development of a dehalogenase-based protein fusion tag capable of rapid, selective and covalent attachment to customizable ligands. *Curr Chem Genomics* 6:55–71.
- Grimm JB, et al. (2015) A general method to improve fluorophores for live-cell and single-molecule microscopy. *Nat Methods* 12(3):244–250, 3, 250.
- Ziegler-Birling CEL, Miyazaki Y, Torres-Padilla M-E (2013) Live visualization of chromatin dynamics with fluorescent TALEs. *Nat Struct Mol Biol* 20:1321–1324.
- Shi X, et al. (2012) Quantitative fluorescence labeling of aldehyde-tagged proteins for single-molecule imaging. *Nat Methods* 9(5):499–503.
- Zijlmans JM, et al. (1997) Telomeres in the mouse have large inter-chromosomal variations in the number of T2AG3 repeats. *Proc Natl Acad Sci USA* 94(14):7423–7428.
- O'Connell MR, et al. (2014) Programmable RNA recognition and cleavage by CRISPR/Cas9. *Nature*.
- Beliveau BJ, et al. (2015) Single-molecule super-resolution imaging of chromosomes and in situ haplotype visualization using Oligopaint FISH probes. *Nat Commun* 6:7147.
- Chen KH, Boettiger AN, Moffitt JR, Wang S, Zhuang X (2015) RNA imaging. Spatially resolved, highly multiplexed RNA profiling in single cells. *Science* 348(6233):aaa6090.
- Hsu PD, et al. (2013) DNA targeting specificity of RNA-guided Cas9 nucleases. *Nat Biotechnol* 31(9):827–832.
- Esvelt KM, et al. (2013) Orthogonal Cas9 proteins for RNA-guided gene regulation and editing. *Nat Methods* 10(11):1116–1121.
- Jinek M, et al. (2012) A programmable dual-RNA-guided DNA endonuclease in adaptive bacterial immunity. *Science* 337(6096):816–821.
- Schneider CA, Rasband WS, Eliceiri KW (2012) NIH Image to ImageJ: 25 years of image analysis. *Nat Methods* 9(7):671–675.
- Janicki SM, et al. (2004) From silencing to gene expression: Real-time analysis in single cells. *Cell* 116(5):683–698.